# Shattering of a liquid drop due to impact

By Ruben D. Cohen

*Department of Mechanical Engineering and Materials Science, Rice University, Houston, Texas 77251, U.S.A.*

Based on energy and entropy principles, a statistical model describing the shattered state of a single spherical liquid drop after being subjected to a relatively sudden but uniform (over the whole surface area of the drop) impact is developed. The problem is addressed from a fundamental standpoint, with the intention of providing a predictive framework for the various modes of breakup and the size and number of droplets produced. Upon neglecting viscous effects, several results in terms of the energy of impact, non-dimensionalized with respect to the surface energy of the drop before impact, are derived. The model is quite simple and straightforward, yet it appears to predict in a fairly consistent manner certain experimental observations that have been made repeatedly in relation to drop breakup in stirred dispersions, by collision, and exposure to shocks.

## 1. Introduction

Owing to its widespread use in industry, the area of drop formation in stirred vessels containing two or more immiscible liquids has received considerable attention in the past few decades. Since the appearance of Hinze's simple, yet powerful theory on the characteristic drop sizes in vigorously agitated dispersions (Hinze 1955), a great number of papers dealing with the same topic have followed. The primary focus of many of these works is set on investigating the formation of drop size distributions under conditions involving mainly breakup (Shinnar 1961; Sprow 1967), coalescence (Muralidhar & Ramkrishna 1988) and simultaneous breakup and coalescence (Cohen 1990*a*).

The literature also contains a lot of work dealing with the details of drop breakup in turbulent flow fields, many of which are directed towards understanding the mechanism of splitting due to fluctuations in pressure and velocity, and also by shear deformation (Hinze 1948*a*, *b*; Delichatsios 1975; Gandhi & Kumar 1990, and references within). Moreover, a number of papers furnish experimental drop size distributions resulting from the collision of water droplets (List *et al.* 1970; McTaggart-Cowan & List 1975; Low & List 1982*a*, *b*), in addition to the characteristic breakup timescale upon exposure to shock or air blast (Komabayasi *et al.* 1964; Simpkins & Bales 1972). Considering all the above, plus the numerous related works not mentioned here, it is a surprise that very few, if any, have yet attempted to provide a predictive model for the size distribution of the 'daughter' droplets formed by the shattering of a single 'mother' drop. An analysis of the problem from this point of view should, therefore, be valuable in widening the scope of knowledge in the area of drop breakup, and the subsequent drop size distributions.

*Proc. R. Soc. Lond.* A (1991) **435**, 483–503
*Printed in Great Britain*

## 2. Model formulation

To begin with, it is necessary to realize that unlike the problem of the breakup of a cylindrical liquid column, which is inherently unstable to infinitesimal disturbances having certain wavelengths, a spherical liquid drop is stable to small non-oscillatory disturbances, and, therefore, at least a finite amount of energy is necessary to cause it to burst. This is due to the fact that a spherical drop of liquid is already at its minimum free energy level, which explains why a critical Weber number (directly related to the impact energy) is required to break it. Hence, a detailed and proper treatment of the breakup of a liquid drop would involve more than the classical method of subjecting it to small disturbances and examining the conditions for their growth.

It therefore follows that a full analytical assessment of this problem would be a formidable task should the conventional approach of solving the fluid mechanics (Navier–Stokes) equations be taken. Nevertheless, it would seem plausible that by using the well accepted energy and entropy principles, one should at least be able to derive certain important characteristics related to the effects of the impact on the state of the droplet sizes after shattering. An analysis of such shall form the primary aim of this paper.

For the sake of simplicity, we assume the mother or parent drop (mother or parent shall refer to the drop before impact) to be stationary and spherical with an initial diameter equal to $d_0$. We also assume that the impact is applied uniformly over the entire surface of the mother drop, so that net momentum transfer is zero. The timescale of the duration of the impact, which can be an important parameter, is discussed in §7.

The impact transfers a total amount of energy, $E_T$, to the drop; all of which is transformed into surface and other forms of energy. It is important to emphasize that we define the impact energy, $E_T$, as the amount that the drop absorbs, and excludes any amount from the original impact that may be partitioned to the surrounding fluid.

It follows from energy conservation that the energies before and after impact are related by

$$E_T + \sigma\pi d_0^2 = E_s + E_R, \tag{1}$$

where $\sigma$ is the interfacial tension, $\pi d_0^2$ is the surface area of the mother drop, $E_s$ is the total surface energy of the resulting daughter droplets, and $E_R$ is the remainder of the energy absorbed by the daughter droplets in other forms, such as kinetic, oscillation, etc. Furthermore, a portion of $E_R$ comprises contributions from the configurational entropy. The reader may refer to Cohen (1990*b*) for order-of-magnitude estimates of this parameter.

Furthermore, it is important to note that all viscous effects are ignored. This carries certain implications, which are discussed later. Also, owing to the thermodynamical nature of the approach, we seek to relate the states before and after breakup, rather than to deal with what actually occurs during breakup. The final aim is, of course, to develop a framework for predicting the various modes of breakup and the size and number of droplets produced after breakup.

According to equation (1), maximum surface energy is achieved by the daughter droplets following impact if $E_R = 0$; in other words, all energy of impact, $E_T$, is absorbed into creating the final surface after shattering. Hence,

$$(E_s)_{max} = E_T + \sigma\pi d_0^2, \tag{2}$$

where $(E_s)_{max}$ represents the maximum total surface energy of the daughter droplets after impact. Likewise, if none of $E_T$ goes into creating any additional surface area (i.e. no breakup after impact), then all the impact energy shall be converted into $E_R$, comprising oscillation and other forms of available energies.

It is necessary now to focus our attention on the size distribution of the daughter droplets after impact. We shall address this first in a preliminary framework, and subsequently apply the results to the general analysis that follows shortly.

Consider the shattering of a spherical liquid drop having an initial diameter equal to $d_0$. Neglecting compressibility effects, mass conservation can be expressed as

$$d_0^3 = \sum_{i=1}^{i_{max}} N_i\, d_i^3, \tag{3}$$

where the left-hand and right-hand sides, respectively, denote before and after impact. In equation (3), $i$ represents the 'class size', which shall be discussed later, and $N_i$ and $d_i$ are the number and diameter of the daughter droplets falling within class size $i$. Also, for convenience, we introduce $d_{min}$ and $d_{max}$ such that

$$d_{min} \equiv d_1 \tag{4a}$$

and

$$d_{max} \equiv d_{i_{max}}, \tag{4b}$$

to represent the minimum and maximum droplet sizes in the distribution after shattering. Consequently, we may express the total surface energy of the daughter droplets as

$$E_s = \sigma\pi \sum_{i=1}^{i_{max}} N_i d_i^2. \tag{5}$$

Upon maximizing the surface energy in (5), in association with the mass constraint of (3), it is easy to prove that for a certain number of daughter droplets, $N^*\,(=\sum_i N_i)$, and for any limited amount of available energy, the size distribution is monodisperse, i.e.

$$d = d^* = \text{const.} \tag{6}$$

Physically, the above means that maximum surface is achieved for any given $N^*$ if all the droplets have equal sizes. Hence, it follows that (3) and (5) can be written as

$$d_0^3 = N^* d^{*3} \tag{7}$$

and

$$(E_s)_{max} = \sigma\pi N^* d^{*2}, \tag{8}$$

respectively, where $(E_s)_{max}$ is the maximum achievable surface energy, which we shall assume to be the same as that introduced earlier in (2).

Upon eliminating $N^*$ from (7) and (8), we obtain

$$d^* = \sigma\pi d_0^3/(E_s)_{max}. \tag{9}$$

However, since $(E_s)_{max}$ is a maximum, then by virtue of (9), $d^*$ must be a minimum. Thus, it is convenient to define the minimum possible drop diameter, $d_{min}$, of the daughter droplets as

$$d_{min}/d_0 \equiv d^*/d_0 = \sigma\pi d_0^2/(E_s)_{max}. \tag{10}$$

Also, eliminating $d^*$ from (7) and (8) yields

$$N^* = [(E_s)_{max}/\sigma\pi d_0^2]^3. \tag{11}$$

Again, because $(E_s)_{max}$ is a maximum, then $N^*$ must also be a maximum by virtue of the above equation. For convenience, therefore, we introduce the maximum possible number of daughter droplets, $N_0$ (for a given $(E_s)_{max}$), as

$$N_0 \equiv N^* = [(E_s)_{max}/\sigma\pi d_0^2]^3. \tag{12}$$

Returning now to (2), which relates $(E_s)_{max}$ to the impact energy, $E_T$, we rewrite (10) and (12), respectively, in the following forms,

$$d_{min}/d_0 \equiv (1+\hat{E}_T)^{-1} \tag{13}$$

and

$$N_0 = (1+\hat{E}_T)^3, \tag{14}$$

where the dimensionless impact energy, $\hat{E}_T$, is defined as

$$\hat{E}_T \equiv E_T/\sigma\pi d_0^2. \tag{15}$$

The relation between $\hat{E}_T$ and the Weber number, *We*, which is a common parameter in drop breakup problems, is derived and discussed in §6.

## 3. General modal development

Figure 1 illustrates the important features of the discussions presented above, namely the limiting size distributions of the daughter droplets achievable upon subjecting a larger parent drop to an impact of energy $E_T$. Case (*a*) represents the situation where all of $E_T$ is converted into surface energy, thereby resulting in a monodisperse fragment size distribution with diameter equal to $d_{min}$. Case (*b*), on the other hand, involves no breakup, and, therefore, no additional surface formation. Consequently, in this case, $E_T$ is fully transformed into $E_R$, comprising kinetic and oscillation energies, among others.

The above reasoning, therefore, points towards the possible existence of daughter droplet size distributions falling anywhere between the two limiting cases, (*a*) and (*b*), shown in figure 1. These intermediate distributions, resulting from equipartitioning of the impact energy over all possible shattered states, should, nevertheless, occur for post-impact surface energies, $E_s$, ranging anywhere between

$$\sigma\pi d_0^2 < E_s < (E_s)_{max}, \tag{16}$$

where $E_s = \sigma\pi d_0^2$ denotes case (*b*), and $E_s = (E_s)_{max}$ represents case (*a*). We now assume that none of the droplets in the subsequent daughter group is smaller than the minimum size, $d_{min}$, as determined by $\hat{E}_T$ through (13). We base this assumption on simple dimensional and physical grounds related to the breakup of inviscid liquid jets by capillary forces where a certain minimum drop size results if breakup is to occur spontaneously due to a destabilizing disturbance.

Hence, in accordance with this assumption, we refer to figure 2 which depicts all the possible size distributions that can be created upon shattering of a parent drop having size $d_0$. Assuming that the smallest possible (primary) droplets, which have diameter $d_{min}$, form the building blocks of all subsequent size distributions, i.e. all other configurations are simply combinations and permutations of the $N_0$ distinguishable primary droplets, we find that for this particular example, where $\hat{E}_T$ is such that $N_0 = 4$ (recall that $N_0$ is related to $\hat{E}_T$ by virtue of (14)), the breakup of a single mother drop should lead to five distinctive categories of size distributions. Of course, all possible combinations must be accounted for since the impact generates random motions within the drop before shattering it.

We should emphasize that although the building block assumption involving

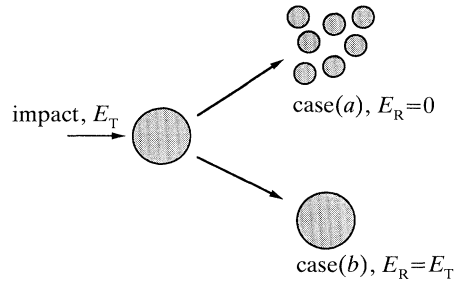


Figure 1. Extreme limits of an impact affecting a single drop. Case ($a$): complete shattering to the state of primary droplets of diameter $d_{min}$. Case ($b$): no shattering, with all of the impact energy being transformed into other forms of energy, except additional surface energy.

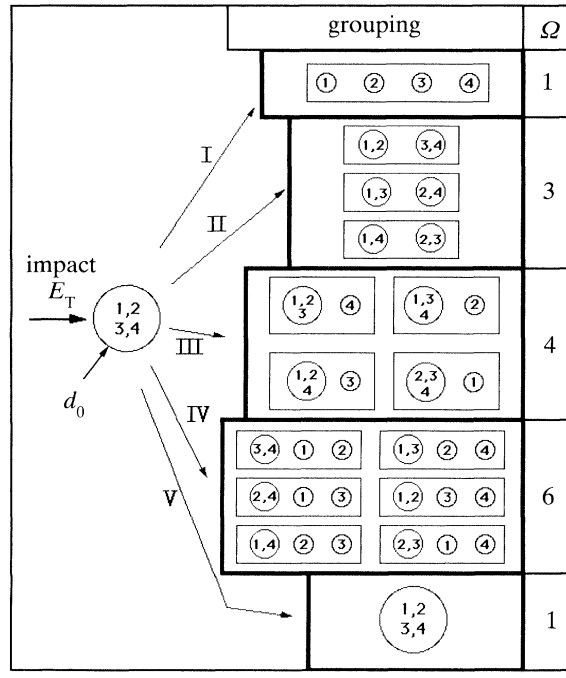


Figure 2. All possible states of shattering of a mother drop of diameter $d_0$ subjected to an impact energy of magnitude $E_T$. Example for $N_0 = 4$.

distinguishable primary elements is obviously more suitable for modelling the formation and breakup of solid particle clusters (Cohen 1990*a*) than of liquid drops, it could very well serve as the foundation for the current statistical approach. Of course, certain implications and weaknesses, some of which shall be addressed later, are expected to arise from this assumption.

In reference to figure 2, we observe that the possible daughter droplet size distributions fall within the five categories, denoted as I to V, described below.

*Category I.* A total of four equal-sized primary droplets each with diameter $d_{min}$.

*Category II.* Two equal-sized droplets each with diameter $2^{\frac{1}{3}}d_{min}$.

*Category III.* A total of two daughter droplets, one with diameter equal to $d_{min}$ and the other with diameter equal to $3^{\frac{1}{3}}d_{min}$.

*Category IV.* A total of three daughter droplets, one with size equal to $2^{\frac{1}{3}}d_{\min}$ and two with diameters equal to $d_{\min}$.

*Category V.* One droplet of size $4^{\frac{1}{3}}d_{\min}$, which is just $d_0$ by virtue of mass conservation.

It is important to note that categories I and V correspond to the limiting cases, (*a*) and (*b*), illustrated in figure 1, and categories II, III and IV, are all the possible intermediate distributions or configurations.

An important outcome of the situation exemplified in figure 2 for $N_0 = 4$ (or $\hat{E}_T = 4^{\frac{1}{3}} - 1$, by means of (14)) concerns the degeneracy associated with each of the five categories. For example, we observe that there is only one way to gain access to each of the categories I and V, whereas categories II, III and IV, respectively, are achievable in three, four and six different ways. The fact that the degeneracy associated with category IV is a maximum simply means that if we conduct the same experiment (i.e. subjecting a liquid drop to an impact of $\hat{E}_T = 4^{\frac{1}{3}} - 1$) many times, then among the samples collected, category IV should be the most prevalent, and, therefore, the most observable.

As a consequence of the above reasoning, it is useful to define a general degeneracy, denoted as $\Omega(N_1, N_2, N_3, \ldots, N_{N_0})$, in order to represent the total number of ways that a parent drop, upon being subjected to impact, could shatter into a group of daughter droplets having a size distribution given by $N_1$ droplets of size $d_{\min}$ (primary droplets), $N_2$ droplets of size $2^{\frac{1}{3}}d_{\min}$, $N_3$ droplets of size $3^{\frac{1}{3}}d_{\min}$, and so on. Returning to figure 2, therefore, we find that $\Omega(4,0,0,0) = 1$, $\Omega(0,2,0,0) = 3$, $\Omega(1,0,1,0) = 4$, $\Omega(2,1,0,0) = 6$, and $\Omega(0,0,0,1) = 1$ pertain to categories I–V respectively.

Derivation of the general expression for the degeneracy, $\Omega$, which should be applicable to any given $N_0$, is based on combinatorial arguments, and for this particular problem it is straightforward but long and, hence, is not included here. It can be shown, however, that $\Omega$ is expressible by

$$\Omega(N_1, N_2, N_3, \ldots, N_{N_0}) = N_0! \Big/ \prod_{i=1}^{i_{\max}} N_i!\,(i!)^{N_i}, \tag{17}$$

which is identical to the one introduced earlier by Cohen (1990*a*) for modelling the steady-state coagulation–breakup process in stirred dispersions.

Based on the proposed building block model illustrated in figure 2, we rewrite (3) as

$$\frac{d_0^3}{d_{\min}^3} = \sum_{i=1}^{i_{\max}} iN_i, \tag{18}$$

where $i$ is the class size, as introduced earlier, or just the droplet size (i.e. the number of primary building blocks of size $d_{\min}$ forming a larger daughter drop of size $d_i$). This is expressible by

$$i = \{d_i/d_{\min}\}^3. \tag{19}$$

Note that (18) is just the mass or volume conservation constraint, which can be written as

$$N_0 = \sum_{i=1}^{i_{\max}} iN_i \tag{20}$$

after combining (10) and (12). The upper limit of the summation, $i_{\max}$, is the largest drop size found in the resulting group of daughter droplets.

The aim now is to search for the most observable or probable daughter droplet size distribution from the general degeneracy expression. This is made possible by maximizing (17) while subjecting it to the constraint of (20). The use of the method of Lagrange multipliers should, therefore, enable us to evaluate the most probable size distribution, $\tilde{N}_i$, of the daughter droplets (Cohen 1990*a*). The final result is

$$\tilde{N}_i = Z^i/i!, \tag{21}$$

where $Z$, which contains the Lagrange multiplier, satisfies the following relation,

$$N_0 = \sum_{i=1}^{i_{\max}} i\frac{Z^i}{i!}, \tag{22}$$

by virtue of (20). To save space, certain steps leading to the derivation of (21) have been omitted here since they are similar to those in Cohen (1990*a*). Nevertheless, we should stress that, for simplicity, (21) was derived using the first two leading terms of the Stirling approximation for $\ln[\tilde{N}_i!]$, based on the assumption that $\tilde{N}_i \gg 1$.

The above can also be approached from another perspective. Upon utilizing the entropy relation (Reif 1965)

$$S = E_{\text{total}}/T + \kappa \ln Q,$$

where $S$, $E_{\text{total}}$, $T$ and $Q$ are the system's entropy, total energy ($E_{\text{total}} = E_{\text{T}} + \sigma\pi d_0^2$), temperature and partition function (i.e. $Q = \Omega \exp[-(E_{\text{R}} + E_{\text{s}})/\kappa T]$) for a given drop size category, and $\kappa$ is Boltzmann's constant, it can be shown that maximizing $\Omega$ is, in fact, identical to maximizing the entropy, $S$, since the sum $E_{\text{total}} = E_{\text{R}} + E_{\text{s}}$ is conserved for all possible subsequent distributions or categories of the daughter droplets, such as those displayed in figure 2.

To evaluate the size of the maximum droplet within the fragments, we define $i_{\max}$ so that it corresponds to

$$\tilde{N}_{i_{\max}} = 1,$$

which leads to

$$Z^{i_{\max}}/i_{\max}! = 1, \tag{23}$$

by virtue of (21). This is reasonable because all $\tilde{N}_i$s must be integers.

## 4. Results

The analysis of §3 led to the most probable daughter droplet size distribution resulting from the shattering of a liquid drop subjected to an impact of dimensionless magnitude $\hat{E}_{\text{T}}$. The final result is the simple expression given by (21), with the distribution parameter, $Z$, satisfying (22).

In principle, therefore, if the impact energy, $E_{\text{T}}$, the size of the parent drop, $d_0$, and the surface tension, $\sigma$, are made available, then one should be able to calculate $N_0$ using (14), and subsequently $Z$ and $i_{\max}$ (by trial and error) from (22) and (23). Finally, with $Z$ and $i_{\max}$ known, $\tilde{N}_i$ can be numerically computed from (21). Alternatively, one may arbitrarily choose $Z$, from which $i_{\max}$, $N_0$ and $\tilde{N}_i$ can be calculated from (23), (22) and (21) respectively.

The latter solution procedure was followed, and the results governing a wide spectrum of $\hat{E}_{\text{T}}$, ranging between $1 < \hat{E}_{\text{T}} < 10^5$, are presented in figure 3 as $Z$ against $\hat{E}_{\text{T}}$. We note that once $Z$ is computed as a function of $\hat{E}_{\text{T}}$, then all of the following can be calculated.

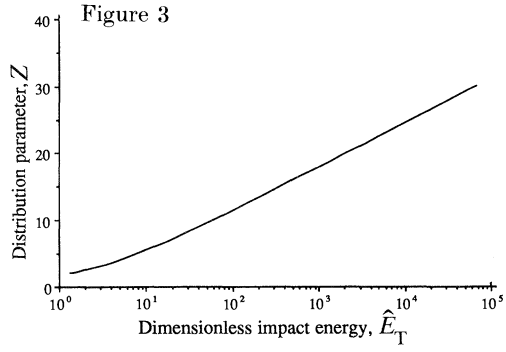


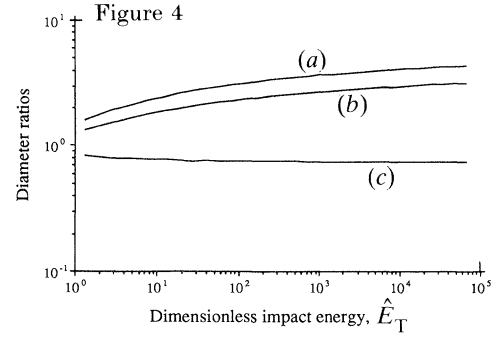


Figure 3. Distribution parameter, $Z$, against the dimensionless impact energy, $\hat{E}_T$.

Figure 4. Diameter ratios against the dimensionless impact energy, $\hat{E}_T$. (*a*) $d_{max}/d_{min}$, (*b*) $d_{32}/d_{min}$ and (*c*) $d_{32}/d_{max}$.

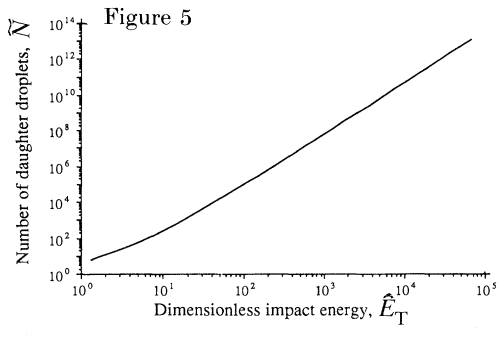


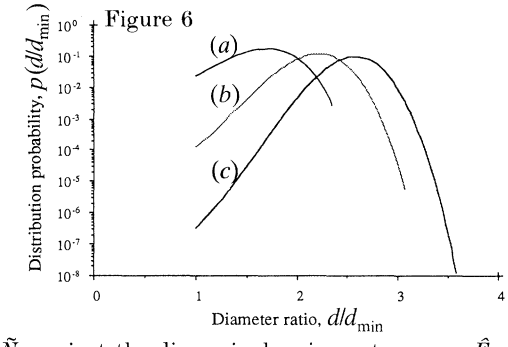


Figure 5. Population of the daughter droplets, $\tilde{N}$, against the dimensionless impact energy, $\hat{E}_T$.

Figure 6. Size distribution probability, $p$, against the diameter ratio, $d/d_{min}$ for (*a*) $\hat{E}_T = 10$, (*b*) $\hat{E}_T = 10^2$ and (*c*) $\hat{E}_T = 10^3$.

1. The maximum diameter ratio, defined by $d_{max}/d_{min}$, is evaluated from (19) using the value of $i_{max}$ obtained from (23). The result is illustrated in figure 4 as $d_{max}/d_{min}$ against $\hat{E}_T$.

2. The total number of daughter droplets, $\tilde{N}$, is simply

$$\tilde{N} = \sum_{i=1}^{i_{max}} \frac{Z^i}{i!}. \tag{24}$$

This is plotted against $\hat{E}_T$ in figure 5. It is worth noting from (24) that for $i_{max} \gg Z$, $\tilde{N}$ approaches $e^Z - 1$.

Regarding figure 5, which shows $\tilde{N}$ to reach values as high as $10^{12}$, we should point out that this represents only the model's prediction extrapolated to very high $\hat{E}_T$. At present, we do not consider this to be a common situation since we are unaware of any type of high-energy systems capable of shattering a single drop into so many fragments. Moreover, it is only fair to speculate that at such high impacts, compressibility effects become significant, thereby affecting the validity of the extrapolations.

3. We define the probability of size distribution, $p(i)$, as

$$p(i) = \tilde{N}_i \Big/ \sum_{i=1}^{i_{max}} \tilde{N}_i, \tag{25}$$

which, by virtue of (21), becomes

$$p(i) = \frac{Z^i}{i!} \Big/ \sum_{i=1}^{i_{\max}} \frac{Z^i}{i!}. \tag{26}$$

This is plotted against the diameter ratio, $d/d_{\min}\,(=i^{\frac{1}{3}})$ in figure 6 for $\hat{E}_T = 10\,(Z \approx 5.49)$, $10^2\,(Z \approx 11.41)$ and $10^3\,(Z \approx 17.85)$, to demonstrate the effect of the magnitude of impact.

4. The Sauter mean diameter, $d_{32}$, computable from the following relation

$$\frac{d_{32}}{d_{\min}} = \sum_{i=1}^{i_{\max}} i \frac{Z^i}{i!} \Big/ \sum_{i=1}^{i_{\max}} i^{\frac{2}{3}} \frac{Z^i}{i!} \tag{27}$$

is also presented in figure 4.

5. Also included in figure 4 is the ratio $d_{32}/d_{\max}$ (obtained from dividing (27) by the recently calculated value of $d_{\max}/d_{\min}$) plotted against $\hat{E}_T$.

6. Other parameters of interest are the ratios $d_{\max}/d_0$ and $d_{32}/d_0$, achieved from multiplying $d_{\max}/d_{\min}$ and $d_{32}/d_{\min}$, respectively, by $d_{\min}/d_0$, which is already available from (13). These, in addition to $d_{\min}/d_0$, are depicted as functions of $\hat{E}_T$ in figure 7.

To summarize, we note the linear relation on log–log scale between the daughter droplet population, $\tilde{N}$, and the dimensionless impact energy, $\hat{E}_T$, in figure 5. Overall, this yields the following scaling relation:

$$\tilde{N} \approx 0.19 \hat{E}_T^{2.84}, \tag{28}$$

which remains valid for large $\hat{E}_T$, i.e. $\hat{E}_T > 20$. Similar scaling expressions at large $\hat{E}_T$, as deduced from figure 7, are

$$d_{\max}/d_0 \approx 2.36 \hat{E}_T^{-0.943} \tag{29a}$$

and

$$d_{32}/d_0 \approx 1.78 \hat{E}_T^{-0.946}, \tag{29b}$$

in addition to (13).

7. The expression for the total surface energy after disintegration becomes

$$\tilde{E}_s = \sigma\pi \sum_{i=1}^{i_{\max}} \frac{Z^i}{i!} d_i^2, \tag{30}$$

which is obtained upon substituting (21) into (5). The tilde on $\tilde{E}_s$ signifies that it is based on the most probable daughter droplet size distribution. In conjunction with (19), the above simplifies to

$$\frac{\tilde{E}_s}{\sigma\pi d_{\min}^2} = \sum_{i=1}^{i_{\max}} i^{\frac{2}{3}} \frac{Z^i}{i!}. \tag{31}$$

Finally, using (13), we obtain

$$\hat{E}_s = \sum_{i=1}^{i_{\max}} i^{\frac{2}{3}} \frac{Z^i}{i!} \Big/ (1 + \hat{E}_T)^2 \tag{32}$$

where the dimensionless surface energy, $\hat{E}_s$, is defined as

$$\hat{E}_s \equiv \tilde{E}_s / \sigma\pi d_0^2 \tag{33}$$

to maintain consistency with $\hat{E}_T$, as given by (15).

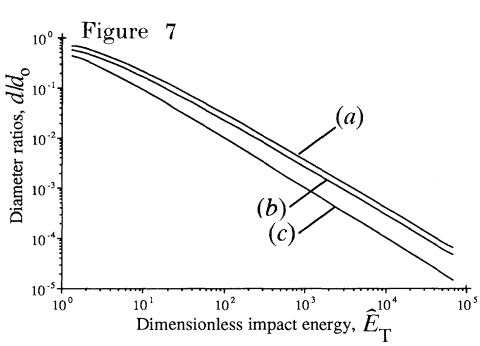


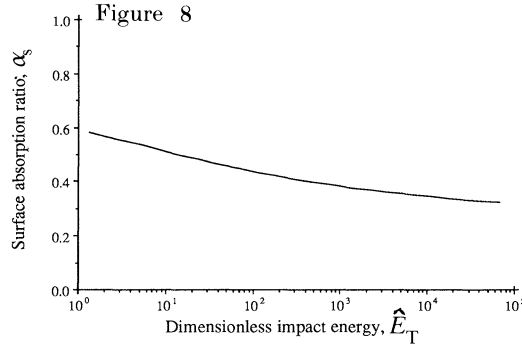


Figure 7. Diameter ratios, $d/d_0$, against the dimensionless impact energy, $\hat{E}_T$: (*a*) $d_{max}/d_0$, (*b*) $d_{32}/d_0$ and (*c*) $d_{min}/D_0$.

Figure 8. Surface energy absorption ratio, $\alpha_s$, against the dimensionless impact energy, $\hat{E}_T$.

In view of the fact that the additional surface energy absorbed into creating the daughter droplets is

$$\Delta\tilde{E}_s = \tilde{E}_s - \sigma\pi d_0^2 \tag{34}$$

it would be beneficial to define the surface energy absorption ratio, $\alpha_s$, as

$$\alpha_s \equiv \Delta\tilde{E}_s/E_T = (\tilde{E}_s - \sigma\pi d_0^2)/E_T \tag{35}$$

or, more simply,

$$\alpha_s \equiv (\hat{E}_s - 1)/\hat{E}_T \tag{36}$$

upon dividing numerator and denominator of (35) by $\sigma\pi d_0^2$.

Therefore, substituting $\hat{E}_s$, which is available from (32), into (36) provides $\alpha_s$. The behaviour of $\alpha_s$ is plotted against $\hat{E}_T$ in figure 8. Evidently, for the range of $\hat{E}_T$ shown, about 30–60 % of the impact energy available is absorbed into creating new surface. Overall the absorption ratio, $\alpha_s$, decreases gradually as $\hat{E}_T$ increases.

8. In addition to the above, the model allows us to evaluate the probability of breakup of a drop, given the dimensionless energy of impact, $\hat{E}_T$. For this, we utilize figure 2 as an example that gives all the probable post-shattering size distributions.

As mentioned earlier, figure 2 represents the case of $N_0 = 4$, i.e. for $\hat{E}_T = 4^{\frac{1}{3}} - 1$ ($= 0.5874$), by means of (14). We find that for this specific example, the probability that the droplet would break upon subjecting it to a dimensionless impact energy of 0.5874 is simply $\frac{14}{15}$; the reason being that there are a total of 15 possible configurations after impact, 14 of which are in shattered states. Hence, for this particular case

$$P_B(\hat{E}_T = 0.5874) = \tfrac{14}{15}. \tag{37}$$

Based on the above, the breakup probabilities for $N_0$ ranging between 1 and 6, corresponding to $0 \leqslant \hat{E}_T \leqslant 0.8171$, respectively, were determined rigorously. The results are tabulated in table 1 and illustrated in figure 9 as $P_B$ against $\hat{E}_T$.

Figure 9 has two noticeable features. First, the integer nature of $N_0$ causes $P_B$ against $\hat{E}_T$ to be discontinuous and step-like at low values of $\hat{E}_T$. For instance, in the limit $0 \leqslant \hat{E}_T < 0.2599$, there should be no breakup, whereas between $0.2599 \leqslant \hat{E}_T < 0.4422$, breakup of the mother drop, if it happens, should be binary, producing two identical daughter droplets. This represents the first mode of breakup, and, according to the model, it is expected to occur with a probability of 50 %. Moreover, between $0.4422 \leqslant \hat{E}_T < 0.5874$, $P_B = 80\,\%$, and so on. Interestingly, this behaviour agrees, at least qualitatively, with the experimental observations of Alusa &

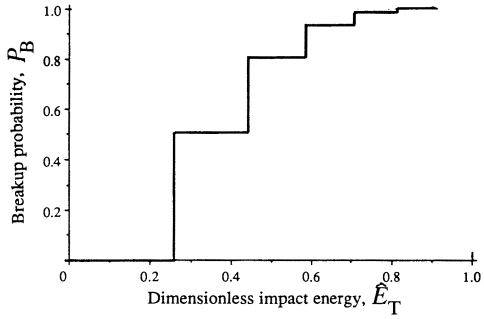


Figure 9. Breakup probability, $P_B$, against the dimensionless impact energy, $\hat{E}_T$.

Table 1. *Tabulated values of* $P_B$ *as a function of* $\hat{E}_T$ *(or* $N_0$*)*

| $N_0$ | $\hat{E}_T = N_0^{\frac{1}{3}} - 1$ | $P_B$ |
|---|---|---|
| 1 | 0 | 0 |
| 2 | 0.2599 | 1/2 |
| 3 | 0.4422 | 4/5 |
| 4 | 0.5874 | 14/15 |
| 5 | 0.7100 | 51/52 |
| 6 | 0.8171 | 202/203 |

Blanchard (1973) concerning the breakup probability near the critical region. Altogether, the model predicts that the discontinuous behaviour should disappear slowly as $\hat{E}_T$ increases, and the curve gradually becomes continuous.

The second feature is that $P_B$ approaches 1 rather quickly when $\hat{E}_T$ reaches only about 0.82. This, for example, means that a drop of water ($\sigma \approx 73$ dyn† cm$^{-1}$ in air) having a diameter of $d_0 = 0.1$ cm, requires an impact energy of at least 1.88 dyn cm$^{-1}$ (i.e. $\hat{E}_T = 0.82$) to shatter it with a probability of over 99.5%.

It should be noted that the treatment of the primary droplets as distinguishable building blocks is an inherent assumption of the model that can raise certain questions regarding its validity. For example, upon considering the case of $N_0 = 3$, we realize that the model is not capable of predicting a shattered state comprising two droplets of equal sizes. This, therefore, deems the breakup probabilities derived here as merely conservative estimates rather than accurate predictions. However, these estimates can furnish lower bound limits that could be fairly reasonable. In addition, the discontinuous dependence of $P_B$ on $\hat{E}_T$, as predicted by the model, should still be maintained even if the model is modified to improve or to correct this rather elementary assumption.

## 5. A remark on some other types of size distributions in attrition processes

We now address the similarities, if any, between the size distribution after shattering of a single spherical droplet derived here (equation (26)) and those of common attrition (breakdown) processes involving solid granules, and even liquid–liquid dispersions. It is well known that quite a few forms of functions, namely the normal, log–normal, and the Rosin–Rammler, can be made to fit the size distributions in these systems. However, some major errors arise due to the fact that these functions are infinite in range, whereas actual distributions are not.

† 1 dyn = $10^{-5}$ N.

Relatively recent works in this area have suggested the possibility of using the beta distribution, instead of the ones mentioned above, for fitting purposes since it avoids the infinite range problem (Popplewell *et al.* 1988; Peleg & Normand 1986). We should also add that the (log of) beta distribution has been successfully applied to aerosol systems (Chang *et al.* 1988).

In relation to the present work, and owing to the fact that the beta distribution can be adjusted to fit the normal distribution very well, it can be concurred within reason, and without having to rely on any detailed calculations, that the beta distribution should also be applicable to the situation studied here. This is because (26) closely resembles the Poisson distribution (since $\sum_i Z^i/i! \approx \exp(Z)$ when $i_{\max} \gg Z > 1$), which, in fact, is a limiting case of the normal distribution.

## 6. Discussion of results and comparison with experiments

The amount of literature on experimental and theoretical works of drop breakup is quite large, and therefore we shall limit this section to a few relevant ones. Before doing so, however, we recall that the current model refers to the word 'impact' generically. Thus, depending on the specific problem being considered, care must be taken to determine the cause of impact so that the correct physical parameters leading to breakup are incorporated.

The works that come to mind at this time, some of which will be used to test the validity of the model, deal with (i) the formation of dispersions in stirred vessels, (ii) disintegration of a drop by exposure to a blast of air (shock exposure), (iii) the collision of liquid droplets (a common occurrence in rainstorms) and (iv) the critical size of a drop falling freely at terminal velocity. All four problems arouse significant interest in a variety of fields ranging from basic engineering to meteorology.

To begin with, however, it is necessary to return to the results tabulated in table 1. Based on the arguments presented in the short section following table 1, the proposed model predicts that the limit of no further breakup occurs at a certain critical impact energy, $E_{\mathrm{Tcr}}$, thereby leading to a certain characteristic critical drop size, $d_{\mathrm{cr}}$. Accordingly, the two parameters, $d_{\mathrm{cr}}$ and $E_{\mathrm{Tcr}}$, are related by the following expression:

$$E_{\mathrm{Tcr}}/\pi\sigma d_{\mathrm{cr}}^2 = 0.2599. \tag{38}$$

The above shall form the basis of much of the discussions presented below. It should be kept in mind, however, that the manner by which $E_{\mathrm{T}}$, and subsequently $E_{\mathrm{Tcr}}$, are defined depends exclusively on the problem under consideration.

### (*a*) *Application to liquid–liquid dispersions*

One of the primary aims of this work is to use the model to explain some of the phenomena that dominate the drop size distributions in agitated liquid–liquid dispersions. As mentioned earlier, the action of stirring can cause pure coalescence, pure breakup, or both coalescence and breakup to occur simultaneously.

The case of stirred dispersions involving only breakup (attrition) of the liquid drops is the most relevant to the proposed model. In such systems, as in all others, the dispersed phase droplet size distribution curve follows a time-dependent profile until, ultimately, steady state is reached. In relation to this work the phenomenon of the evolution to steady state can be viewed as the shattering of each individual drop to the point where the subsequent daughter droplets are too small to break: in

other words, the breakup probability becomes identically equal to zero. In fact, the work of Hinze (1955), which laid the framework for the characteristic steady-state drop size in isotropic turbulence, forms the basis for this point of view.

The critical impact energy, $E_{\mathrm{Tcr}}$, for this particular problem can be determined if the mean-squared velocity fluctuation, $\langle v^2 \rangle$, across the drop is known. Realizing that within a constant of order unity, $\frac{1}{2}\langle v^2 \rangle$ represents approximately the impact energy per unit mass of the continuous phase (since the impact energy is provided by the turbulence in the continuous phase) acting on a drop of volume $\frac{1}{6}\pi d_{\mathrm{cr}}^3$, then

$$E_{\mathrm{Tcr}} = \tfrac{1}{2}\langle v^2 \rangle \rho_{\mathrm{c}} \tfrac{1}{6}\pi d_{\mathrm{cr}}^3, \tag{39}$$

where $\rho_{\mathrm{c}}$ is the density of the continuous phase. Now, upon defining the critical Weber number, $We_{\mathrm{cr}}$, sufficient to cause the drop to break, as (Hinze 1955)

$$We_{\mathrm{cr}} = \rho_{\mathrm{c}} \langle v^2 \rangle d_{\mathrm{cr}}/\sigma \tag{40}$$

we obtain

$$We_{\mathrm{cr}} = 12\hat{E}_{\mathrm{Tcr}} = (12)(0.2599) \approx 3.12 \tag{41}$$

upon combining (38)–(40). Interestingly, this compares well with Hinze's result of $We_{\mathrm{cr}} = 1.18$. Also, more generally, it follows from (41) that the Weber number, $We$, can be related to the dimensionless energy of impact, $\hat{E}_{\mathrm{T}}$, by

$$We = 12\hat{E}_{\mathrm{T}}. \tag{42}$$

Alternatively, one can incorporate the relation for homogeneous turbulence (Batchelor 1951)

$$\langle v^2 \rangle \approx 2(\epsilon d_{\mathrm{cr}})^{\frac{2}{3}} \tag{43}$$

as used by Hinze (1955), where $\epsilon$ is the Kolmogorov turbulent energy dissipation rate per unit mass of the continuous phase. Substituting the above into (39), and the result into (38), yields

$$d_{\mathrm{cr}}(\rho_{\mathrm{c}}/\sigma)^{\frac{3}{5}}\epsilon^{\frac{2}{5}} = [(6)(0.2599)]^{\frac{3}{5}} = \text{const.} = 1.306. \tag{44}$$

In correlating his model with previous experimental results, Hinze (1955) obtained an expression identical to the one given above, however, a value of 0.725 for the constant was generated by data fitting. Although Hinze's correlation and his use of the data were later challenged by Sleicher (1962), we find that good agreement between our result and Hinze's is obtained, especially considering that our model does not use any empirical parameters.

It also follows from the model that if the initial drop diameter, $d_0$, is greater than $d_{\mathrm{cr}}$, (44) becomes

$$d_0(\rho_{\mathrm{c}}/\sigma)^{\frac{3}{5}}\epsilon^{\frac{2}{5}} > 1.306. \tag{45}$$

The inequality in (45) suggests that breakup must proceed up to the point where $d_{\mathrm{cr}}$ is reached, i.e. in an actual dispersion, the parent drop of initial size $d_0$ periodically shatters until, ultimately, its largest daughter droplet approaches $d_{\mathrm{cr}}$, thereby satisfying (44).

On the other hand, if the left-hand side of (45) is less than 1.306 (which occurs when $d_0 < d_{\mathrm{cr}}$), the current model predicts, by virtue of the results presented in figure 9, a zero breakup probability, and, therefore, no further breakup of the parent drop. This is consistent with the observation that by continuously stirring a dispersion in which the largest drops are comparable with or smaller than the critical size, a steady-state size distribution is achieved, although the amount of energy being added to the system becomes infinitely larger than the interfacial area between the phases.

In addition to the above, it would be helpful to apply some actual numbers available from liquid–liquid dispersion experiments to test the validity of (44). For example, if we use $\epsilon \geqslant 3000$ cm$^2$ s$^{-3}$, $\rho_c \approx 1$ g cm$^{-3}$ and $\sigma \approx 20$ dyn cm$^{-1}$, which are very typical (see, for example, Nishikawa *et al.* 1987, among many others), we obtain from (44) that

$$d_{cr} = \frac{1.306}{(\rho_c/\sigma)^{\frac{3}{5}}\epsilon^{\frac{2}{5}}} = \frac{1.306}{(1/20)^{0.6}\,3000^{0.4}} \approx 0.32 \text{ cm}, \tag{46}$$

which is an order of magnitude larger than the typical experimental values of about 0.03 cm. The discrepancy, which apparently applies to many of the liquid–liquid experiments that we have examined (see also, for example, Calderbank 1958), can be explained by the fact that the breakup of drops occurs very likely in the regions close to the stirrer blades, where the local value of $\epsilon$ can be larger than the average dissipation rate by as much as 70 times (Cutter 1966). Therefore, incorporating a factor of 70 into (46) yields

$$d_{cr} = \frac{1.306}{(1/20)^{0.6}\,(70\times 3000)^{0.4}} \approx 0.06 \text{ cm}, \tag{47}$$

which is in much better agreement with typical experimental $d_{cr}$s than (46) suggests.

Another important outcome of the model is that although the parameters $d_{max}/d_{min}$ and $d_{32}/d_{min}$ are evidently affected by the dimensionless impact energy (see figure 4), the ratio $d_{32}/d_{max}$ is weakly influenced by $\hat{E}_T$, and therefore by the Weber number, *We*. As a matter of fact, the ratio can be considered to be practically a constant, approximately equal to 0.74, over the wide range of $\hat{E}_T$ investigated. It is actually possible to show that $d_{32}/d_{max}$ tends to about 0.717 as $\hat{E}_T \to \infty$, i.e. $N_0 \to \infty$ (Cohen 1990*a*).

In light of the above, we should point out that numerous experimental studies concerning measurements of the steady-state drop size distributions in stirred liquid–liquid dispersions have led to similar conclusions. The values of the ratio $d_{32}/d_{max}$ measured from whole dispersions have been reported in the literature as constants ranging between 0.38 and 0.60 (Sprow 1967; Nishikawa *et al.* 1987; Godfrey *et al.* 1989, among others). If we assume that the overall droplet size distribution in a dispersion reflects that of the breakup of an individual drop, then the quantitative discrepancy between our results and the experimental data may be caused by the fact that the experimental measurements are averages taken over a large number of parent drops, which, in many cases, were fairly polydisperse. In addition, of course, the flow field inhomogeneities and viscosity effects in the actual experiments, aside from the very simplistic analysis taken here must not be overlooked. Nonetheless, although the differences are not small, they do fall within reasonable bounds.

It is noted that the formation of liquid–liquid dispersions in turbulent pipe flow has also been investigated (Sleicher 1962; Sleicher & Paul 1965). Although the use of Hinze's formulation (1955), similar to our (44), was strongly questioned by Sleicher (1962), we find that the calculated critical drop diameters (using (44)) are of the order of 0.4 cm, which are in very good agreement with the experimental measurements. It should be mentioned that to carry out these calculations, we computed the relation between $\epsilon$ and the Reynolds number using the experimental results of Laufer (1954).

### (*b*) *Shattering of a liquid drop by exposure to an air blast*

The literature also contains a great deal of work on the breakup of liquid drops exposed to sudden blasts of a gas. To apply our model to such processes, we must appropriately define the relation between the energy of impact, $E_T$ (which is to be implemented in the current model) and what causes it.

Because the moving continuous phase, which could be either liquid or gas, is the sole source of energy, then the energy of impact transferred to the drop can be reasonably modelled as the quantity $\frac{1}{2}\rho_c U_c^2$, acting on the drop of volume, $\frac{1}{6}\pi d_0^3$. Thus, we express

$$E_T = \rho_c \tfrac{1}{2} U_c^2 \tfrac{1}{6}\pi d_0^3, \tag{48}$$

where $U_c$ is the velocity of the gas, being the continuous phase. This formulation for $E_T$ is consistent with that of (39). However, the factor of 12 may not necessarily be the same because the fluid mechanics are different.

Based on the above, therefore, the Weber number, which is defined by $\rho_c U_c^2 d_0/\sigma$, becomes identical to (42). For the same reason, the critical Weber number for such processes should correspond to (41), thereby giving a $We_{cr} \approx 3.12$ for breakup by exposure to shock. Considering the simplicity of the present approach, the theoretical value of 3.12 compares well with the experimental results ranging between 6.5 (Clift *et al.* 1978) and 13 (Hinze 1955). At this time we believe the reason for the discrepancy to be that (*a*) the exact details of the breakup mechanisms, in terms of the fluid mechanics, are very different for the two cases; from which it follows that (*b*) the same factor of 12 (in (39) and (48)), as indicated above, may not be applicable to both situations, and (*c*) in such instances, $\hat{E}_{Tcr} > 0.2599$ because, according to photographic evidence (Hinze 1955), the breakup mode is greater than binary. In any case, the consistency of the results points clearly towards the fact that the natures of the breakup in both problems, although macroscopically different, originate from the energy conservation principle.

In reference to the daughter drop size distributions after breakup, a brief comparison of the predictions of our model, using (48), with the experiments of Komabayasi *et al.* (1964) conducted at $U_c \approx 10$ m s$^{-1}$ (not shown here), suggests that the present work underestimates the number of fragments produced by a factor of about 5 to 10. In addition, the experimental distributions of the daughter droplets look different to our model prediction (figure 6): the difference being that (*a*) the theoretical distributions are much narrower than the ones measured, and (*b*) contrary to figure 6 of this work, their distributions have no maxima. The first one mentioned, which concerns their wider distributions, can be attributed to, among other possibilities, the formation of a neck and its breakup into many fine particles, thereby leading to a wider size distribution (Alusa & Blanchard 1973). One major experimental result, however, which compares favourably with this work is that $\tilde{N}$ was empirically found to be proportional to $d_0^3$, whereas the model ((28), with the aid of (48)) yields $\tilde{N} \propto d_0^{2.84}$.

Studies involving breakup timescales have also been conducted. Noteworthy of mention is the work of Simpkins & Bales (1972) which, more or less, concludes that the breakup time is on the order of the deformation timescale. The timescale for breakup, and its implications to our work, shall be discussed further in §7.

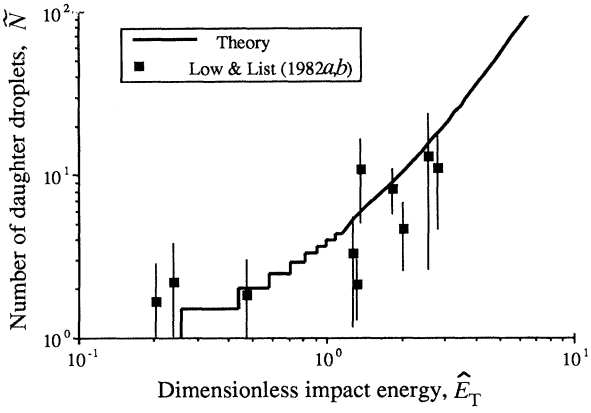


Figure 10. Population of the daughter droplets, $\tilde{N}$, against the dimensionless impact energy, $\hat{E}_T$, at low energies. The squares are the data of Low & List (1982*a*, *b*), and the solid line is the prediction of the proposed model.

### (*c*) *Shattering due to collision of drops*

A major factor limiting the size distribution of raindrops has been determined to be the collision of water droplets. Hence, the problem of drop breakup by collision has found a special niche in the field of meteorology.

In relating the predictions of our model with some existing experiments on collision of water drops ($\sigma \approx 73$ dyn cm$^{-1}$), we refer to the work of Low & List (1982*a*, *b*), which provides data on the effect of the energy of collision on the total number of daughter droplets, $\tilde{N}$, produced. A comparison of their results, in terms of $\tilde{N}$ against $\hat{E}_T$, with our prediction is displayed in figure 10. Figure 10 is just figure 5, but focuses on the lower values of $\hat{E}_T$. The discontinuous nature of breakup in this region, which has been explained earlier (see, for example, figure 9, and the explanation following table 1), is clearly evident.

We should mention that the experiments of Low & List (1982*a*, *b*) involve collisions between two parent drops of unequal sizes, $d_{01}$ and $d_{02}$. Assuming that the two drops coalesce before the final mass disintegrates, $\hat{E}_T$ can then be reasonably expressed as

$$\hat{E}_T = \frac{E_{coll} + \sigma\pi\{(d_{01}^2 + d_{02}^2) - (d_{01}^3 + d_{02}^3)^{\frac{2}{3}}\}}{\sigma\pi(d_{01}^3 + d_{02}^3)^{\frac{2}{3}}},$$

where $E_{coll}$ is the collision energy, which is available from their data, and the quantity $\sigma\pi\{(d_{01}^2 + d_{02}^2) - (d_{01}^3 + d_{02}^3)^{\frac{2}{3}}\}$ is the energy gained from coalescence. Also, in the range of $\hat{E}_T < 1$ (where the discontinuities are most prominent), equation (24) loses its accuracy since it was derived for the continuous region, i.e. $\hat{E}_T > 1$. Hence, for the lower values of $\hat{E}_T$ shown in figure 10, $\tilde{N}$ was calculated rigorously by averaging the number of fragments, $(\tilde{N})_k$, belonging to category $k$, over all the categories, i.e.

$$\tilde{N} = \sum_k (\tilde{N})_k \Omega_k / \sum_k \Omega_k,$$

where $\Omega_k$ is the degeneracy of category $k$. Applying the above to figure 2, for example, yields $\tilde{N}$ (for $\hat{E}_T = 0.5874$ or $N_0 = 4$) to be approximately 2.47.

The scatter that appears in the experimental data as error bars, is caused by the presence of the three different modes of breakup, classified as filaments, sheets and

discs. Overall the agreement is good, considering that the theory does not contain any adjustable parameters. Needless to say, however, there is need for more data before any conclusive claims can be made.

In reference to the fragment sizes, we note that the experimental distributions (not shown here) of Low & List (1982*a*, *b*) are wider than ours. From their data, for example, the ratios of $d_{\max}/d_{\min}$ range between 4 and 6, whereas our model predicts values of 2.5 and less, as depicted in figure 4 for lower impact energies. Assuming that the model described here is valid, we can only speculate that the wider distributions in their experiments may have been caused by having two drops of unequal sizes (different by a factor of greater than 2) colliding to produce the daughter droplets. For this reason, therefore, quantitative comparisons with their daughter drop size distributions are not possible.

### (*d*) *Breakup of a drop falling at terminal velocity*

A liquid drop having density $\rho_d$ and falling at its terminal velocity in a gas or another liquid of density $\rho_c$ can also shatter. This problem is in many ways similar to breakup by exposure to shock.

Methods for predicting the critical diameter in such situations have typically consisted of stability analyses of surface waves, a brief outline of which can be found in Clift *et al.* (1978). In short, the critical drop diameter is given as a function of the system parameters by the following expression

$$d_{cr} \approx 4\sqrt{(\sigma/g\,\Delta\rho)}, \tag{49}$$

where $\Delta\rho \equiv \rho_d - \rho_c$.

To predict the critical diameter from an energy point of view, we return to (48) with $U_c$ being the terminal speed. Further, we incorporate the expression

$$C_D = \tfrac{1}{6}\Delta\rho\pi d_{cr}^3\, g/\rho_c \tfrac{1}{2}U_c^2\,\pi\tfrac{1}{4}d_{cr}^2, \tag{50}$$

where $g$ is the gravitational acceleration and $C_D$ is the drag coefficient. Obviously, the numerator is just the buoyancy force.

Within reasonable accuracy, $C_D$ is nearly constant and equal to about 0.5 for a solid sphere, whereas for a liquid drop, a different value of $C_D$, not much different from 0.5, applies. For simplicity, however, we shall use 0.5 for what follows next.

Substituting (48) into (50), along with a value of $\hat{E}_{Tcr} \approx 1$, yields

$$d_{cr} \approx 2.1\sqrt{(\sigma/g\,\Delta\rho)}, \tag{51}$$

which is consistent with (49), but different by a factor of about 2. It should be mentioned that for this case, $\hat{E}_{Tcr} \approx 1$ is more appropriate than 0.2599 (from equation (38)) because, as indicated earlier, photographic evidence points towards breakup into more than two droplets. The validity of (51) can, nonetheless, be realized after noting that some of the experimental $d_{cr}$s, which are available from table 12.3 of Clift *et al.* (1978), are indeed comparable with our prediction, even with the difference of the factor of 2 present.

## 7. Limitations of the model and conclusions

By means of a statistical approach combined with entropic and energetic considerations, a simple model for the shattering of a single liquid drop subjected to a relatively sudden but uniform impact is introduced. Based on the analysis

presented, several conclusions, many of them having certain fundamental implications in the area of drop size distributions in stirred liquid–liquid dispersions, drop breakup due to collisions, and by exposure to air blasts, are discussed.

One of the features of the model is that it is capable of providing within reasonable accuracy, an estimate of the critical Weber ($We_{cr}$) numbers necessary for drop breakup due to shocks and in stirred liquid–liquid systems, without really the need for any major empirical or adjustable parameters. For example, the critical Weber number, $We_{cr}$, obtained here, which leads to a binary breakup of the initial drop, agrees satisfactorily with the value of 1.18 reported by Hinze (1955) for dispersions. For disintegration following sudden blasts, however, a critical Weber number based on a mode of breakup greater than binary (i.e. $\hat{E}_T \approx 1$) would be more appropriate. Furthermore, the model leads to the prediction of the experimental observation that in a stirred vessel, the ratio $d_{32}/d_{max}$ is constant, independent of all other system parameters, such as stirring rate (related to the impact energy or Weber number), density, surface tension, etc.

To this point we have demonstrated that the method yields, at least qualitatively, certain well-known experimental behaviours. It is, nevertheless, important to point out that one of its major limitations is that no account of viscous effects is made, i.e. the model assumes that no portion of the impact energy dissipates into viscous losses during shattering. These viscous losses, for instance, are generated by the random internal motions imparted to the drop by the initial impact, which yield all the possible arrangements of the building blocks in the shattered states, as exemplified in figure 2.

It should, consequently, be convenient to implement a dimensionless parameter to examine the importance of viscous losses in relation to the momentum and surface tension effects during the breakup process. Through order-of-magnitude arguments this can be carried out by considering conservation of energy,

$$E_T \sim \Delta E_s + E_R + \Phi_d T_B, \tag{52}$$

where the previously defined parameters, $\Delta E_s (= E_s - \sigma\pi d_0^2)$ and $E_R$, denote the increase in surface energy and other types of energies, respectively, whereas $\Phi_d$ is the energy dissipation rate within the drop, and $T_B$ is the timescale of breakup. Note that in the absence of the dissipation term, which is given above by $\Phi_d T_B$, we recover (1) on which this work is based. Hence, we must enforce the inequality

$$\Phi_d T_B / E_T \ll 1 \tag{53}$$

for (1) to apply.

Furthermore, we can scale the internal dissipation rate, $\Phi_d$, as

$$\Phi_d \approx \mu_d V^2 d_0, \tag{54}$$

where $V$ is the velocity of the deformation of the drop just before shattering. Substituting (54) into (53) yields

$$T_B \ll E_T / \mu_d V^2 d_0, \tag{55}$$

which represents the inequality that $T_B$ must satisfy.

To obtain the deformation velocity, $V$, we scale the internal stress, $\tau$, with $E_T/d_0^3$ by means of dimensional analysis, and express

$$\tau \equiv E_T / d_0^3 \approx \mu_d V / d_0 + \rho_d V^2. \tag{56}$$

The above simply implies that, in general, the internal stresses are generated mainly by viscous and inertial forces. Again, however, owing to the fact that inertial forces must dominate in our formulation, i.e. $\mu_d V/d_0 \ll \rho_d V^2$, equation (56) becomes

$$E_T/d_0^3 \approx \rho_d V^2 \tag{57}$$

from which we compute the deformation velocity scale as

$$V \approx \sqrt{(E_T/\rho_d d_0^3)}. \tag{58}$$

Where viscous forces dominate inertia the relation is expected to be different from equation (58) (Levich 1962).

Finally, substituting (58) into (55) yields

$$T_B \ll d_0^2/\nu_d, \tag{59}$$

where $\nu_d (\equiv \mu_d/\rho_d)$ is the kinematic viscosity of the drop. Note that the quantity $d_0^2/\nu_d$ is just the viscous diffusion time within the drop. Thus, for liquid–liquid dispersions where typically $\nu_c \approx \nu_d$, the breakup timescale, $T_B$, must be less than the turbulence timescale, $d_0^2/\nu_c$, which can also be viewed as the duration of the external force or impact (Delichatsios 1975).

Furthermore, one may assume that the breakup timescale, $T_B$, is on the order of the deformation timescale (Delichatsios 1975). From this it follows that

$$T_B \sim d_0/V, \tag{60a}$$

which becomes

$$T_B \sim \sqrt{(\rho_d d_0^3/\sigma \hat{E}_T)} \tag{60b}$$

upon utilizing (58) and (15). It is interesting to note that the above is different from the natural oscillation time for a spherical drop (Lamb 1945) by a factor of $\hat{E}_T^{-\frac{1}{2}}$.

Finally, substituting (60*b*) into (59) yields

$$N_{vi}/\sqrt{\hat{E}_T} \ll 1, \tag{61}$$

where the viscosity number is

$$N_{vi} \equiv \mu_d/\sqrt{(\rho_d \sigma d_0)}, \tag{62}$$

as discussed by Hinze (1955). Within a constant of order one, (61) can be written as

$$N_{vi}/\sqrt{We} \ll 1, \tag{63}$$

after utilizing the relation between $\hat{E}_T$ and $We$ that is available from (42). Hence, since $We$ must always be greater than, or at least equal to unity to ensure drop breakup, then (63) is just a modification of the original restriction of $N_{vi} \ll 1$ (Hinze 1955) should the drop shatter at a Weber number greater than one.

Consequently, if, in relation to the present model, (63) is satisfied, then the predicted results should be valid, otherwise the model is expected to fail. To provide an idea of the magnitude of the left-hand side of (63) in typical liquid–liquid dispersions, we implement such values as $\mu_d \approx 0.01$, $\rho_d \approx 1$, $\sigma \approx 20$ and $d_0 \approx 0.1$, all in g-cm-s units, and obtain $N_{vi}/\sqrt{We} \approx 0.007 \ll 1$ for $\sqrt{We} \approx 1$. This lies well within the bounds of our model.

Again, regarding viscosity effects, the model assumes that following impact, the drop, while undergoing breakup, encounters minimal resistance from the continuous phase surrounding it. This requires that the ratio $\mu_d/\mu_c$, where $\mu_c$ is the continuous phase viscosity, be greater than unity. As noted by Hinze (1955), a ratio of $\mu_d/\mu_c > 1$

(which is true in the case of many liquid–liquid dispersion processes, and, of course, in exposure of liquid drops to air blasts) yields daughter droplets which have somewhat narrow size distributions. This observation agrees qualitatively with the results of this work, as concluded from figure 4 where the predicted values of $d_{\max}/d_{\min}$ (which lie between approximately 1 and 4 for a wide range of impact energies) indicate relatively narrow distributions.

An additional limitation of the model lies in its inherent assumption that the primary droplets, which are the distinguishable building blocks, lead to the size distributions of the daughter droplets. As discussed earlier, this should yield conservative but fairly reasonable estimates of the behaviour. Nevertheless, satisfactory agreement with the experimental data shown in figure 10 is obtained.

Concerning the predicted size distributions of the daughter droplets, the reasonable qualitative agreement with the data of Low & List (1982*a*, *b*) and McGowan-Taggart & List (1972), which are not shown here, must not be overlooked. But because comparisons with experiments are few and qualitative at this time, no conclusive claims about the validity of the model can be made yet. Thus, the success of (26), which was derived on the basis of maximizing the 'distribution entropy', remains open to further scrutiny.

In conclusion, a detailed analysis of liquid drop disintegration by impact is a very complicated phenomenon, encompassing far more than the simplistic view presented here. The vast differences in the mechanism, especially the fluid mechanics of breakup related to each of the cases considered above makes this matter even more formidable. What this work provides, however, is an elementary attempt to explain some of the general and well known characteristics related to this problem. It simply proposes another perspective that can add a little more to the present knowledge of this area. In spite of its simplicity and limitations, we have, none the less, demonstrated that the model does have some potentials. Therefore, looking into possibilities for future extensions and modifications, such as incorporating momentum conservation and viscous effects into the analysis, might be worthwhile.

Partial support from the Texas Energy Research in Applications Program (ERAP) grant no. 003604-019 is acknowledged.

## References

Alusa, A. L. & Blanchard, C. 1973 Drop-size distributions produced by the breakup of large drops under turbulence. *J. Rech. Atmos.* **7**, 1–9.

Batchelor, G. K. 1951 Pressure fluctuations in isotropic turbulence. *Proc. Camb. Phil. Soc.* **47**, 359–374.

Calderbank, P. H. 1958 Physical rate processes in industrial fermentation – Part I. *Trans. Instn chem. Engrs* **36**, 443–463.

Chang, Y., Han, R. J., Pearson, C. L., Runyan, M. R. & Gentry, J. W. 1988 Applications of the log beta-distribution to the evolution of aerosol growth. *J. Aerosol Sci.* **19**, 879–882.

Clift, R., Grace, J. R. & Weber, M. E. 1978 *Bubbles, drops and particles*. New York: Academic Press.

Cohen, R. D. 1990*a* Steady-state cluster size distribution in stirred suspensions. *J. chem. Soc. Faraday Trans.* **86**, 2133–2138.

Cohen, R. D. 1990*b* Entropic and energetic factors in steady-state coagulation-breakup processes. *Powder Technol.* **63**, 261–263.

Cutter, L. A. 1966 Flow and turbulence in a stirred tank. *A.I.Ch.E. J.* **12**, 35–45.

Delichatsios, M. A. 1975 Model for the breakup rate of spherical drops in isotropic turbulent flows. *Phys. Fluids* **18**, 622–623.

Gandhi, K. S. & Kumar, R. 1990 An elongational flow model for drop breakage in stirred turbulent dispersions. *Chem. Engng Sci.* **45**, 2998–3001.

Godfrey, J. C., Obi, F. I. N. & Reeve, R. N. 1989 Measuring drop size in continuous liquid–liquid mixers. *Chem. Engng Progress* **85**, 61–69.

Hinze, J. O. 1948*a* Forced deformations of viscous liquid globules. *Appl. Sci. Res.* A **1**, 263–272.

Hinze, J. O. 1948*b* Critical speeds and sizes of liquid globules. *Appl. Sci. Res.* A **1**, 273–288.

Hinze, J. O. 1955 Fundamentals of the hydrodynamic mechanism of splitting in dispersion processes. *A.I.Ch.E. J.* **1**, 289–295.

Komabayasi, M., Gonda, T. & Isono, K. 1964 Life time of water drops before breaking and size distribution of fragment droplets. *J. met. Soc. Japan* **42**, 330–340.

Lamb, H. 1945 *Hydrodynamics.* New York: Dover.

Laufer, J. 1954 Structure of turbulence in fully developed pipe flow. *U.S. Natl Advis. Comm. Aeron.* Rep. no. 1174.

Levich, V. G. 1962 *Physicochemical hydrodynamics.* New York: Prentice-Hall.

List, R., MacNeil, C. F. & McTaggart-Cowan, J. D. 1970 Laboratory investigations of temporary collisions of raindrops. *J. geophys. Res.* **75**, 7573–7580.

Low, T. B. & List, R. 1982*a* Collision, coalescence, and breakup of raindrops. Part I: Experimentally established coalescence efficiencies and fragment size distributions in breakup. *J. Atmos. Sci.* **39**, 1591–1606.

Low, T. B. & List, R. 1982*b* Collision, coalescence, and breakup of raindrops. Part II: Parameterization of fragment size distributions. *J. Atmos. Sci.* **39**, 1607–1618.

McTaggart-Cowan, J. D. & List, R. 1975 Collision and breakup of water drops at terminal velocity. *J. Atmos. Sci.* **32**, 1401–1411.

Muralidhar, R. & Ramkrishna, D. 1988 Coalescence phenomena in stirred liquid–liquid dispersions. In *Proc. Sixth Euro. Conf. on Mixing.* Pravia, Italy.

Nishikawa, M., Mori, F. & Fujiedo, S. 1987 Average drop size in a liquid–liquid phase mixing vessel. *J. chem. Engng Japan* **20**, 83–88.

Peleg, M. & Normand, M. D. 1986 Simulation of size reduction and enlargement processes by a modified version of the beta distribution function. *A.I.Ch.E. J.* **32**, 1928–1930.

Popplewell, L. M., Campanella, O. H., Normand, M. D. & Peleg, M. 1988 Description of normal, log-normal and Rosin-Rammler-particle populations by a modified version of the beta distribution function. *Powder Technol.* **54**, 119–125.

Reif, F. 1965 *Fundamentals of statistical and thermal physics.* New York: McGraw-Hill.

Shinnar, R. 1961 On the behaviour of liquid dispersions in mixing vessels. *J. Fluid Mech.* **10**, 259–275.

Simpkins, P. G. & Bales, E. L. 1972 Water drop response to sudden accelerations. *J. Fluid Mech.* **55**, 629–639.

Sleicher, C. A. 1962 Maximum stable drop size in turbulent flow. *A.I.Ch.E. J.* **8**, 471–477.

Sleicher, C. A. & Paul, H. I. 1965 The maximum stable drop size in turbulent flow: Effect of pipe diameter. *Chem. Engng Sci.* **20**, 57–59.

Sprow, F. B. 1967 Distribution of drop sizes produced in turbulent liquid–liquid dispersion. *Chem. Engng Sci.* **22**, 435–442.

*Received 14 January 1991; accepted 27 June 1991*